

## Theoretical Investigation of the Reaction of $\text{Co}^+$ with OCS

Chengbu Liu,\* Dongju Zhang, and Wensheng Bian

College of Chemistry and Chemical Engineering, Shandong University,  
Jinan, 250100, People's Republic of China

Received: March 18, 2003; In Final Form: August 9, 2003

The reaction of  $\text{Co}^+$  with OCS on both triplet and quintet surfaces has been investigated at the B3LYP level of theory of density functional theory with the standard 6-311+G(d) basis set. The object of this investigation was the elucidation of the reaction mechanism. The calculated results indicate that both the C–S and C–O bond activations proceed via an insertion-elimination mechanism. Although the direct sulfur and oxygen atom abstractions by  $\text{Co}^+$  might contribute to the formations of  $\text{CoS}^+$  and  $\text{CoO}^+$ , the tight transition state structures were not found in the present calculations. Intersystem crossing between the triplet and quintet surfaces may occur along both the C–S and C–O bond activation branches. The ground states of  $\text{CoS}^+$  and  $\text{CoO}^+$  were found to be quintets, whereas  $\text{CoCO}^+$  and  $\text{CoCS}^+$  have triplet ground states. The C–S bond activation is energetically much more favorable than the C–O bond activation. All theoretical results are in line with early experiments.

### Introduction

The chemistry of transition-metal sulfides plays an important role in various research areas of chemistry, biology, and material science.<sup>1–3</sup> In many biological systems, it has been found that sulfur coordination is necessary for the functioning of numerous biological transition metal centers.<sup>4,5</sup> In industrial areas, considerable attention has been focused on the role of sulfur-containing transition metal complexes in catalyst poisoning and hydrodesulfurization.<sup>6</sup>  $\text{CS}_2$  and OCS are important sulfur-transfer reagents, which have recently been considered as possible sulfur sources for preparing thin layers of semiconductor materials.<sup>7</sup> These two closely related molecules (isovalent linear triatomic molecules) have been shown to be very reactive toward transition-metal centers and can undergo a variety of reactions such as coordination, insertion, dimerization, or disproportionation.<sup>2,8–9</sup> Recently, guided ion beam mass spectrometry studies on the reactions of the first row transition metal cations (from Sc to Zn) with  $\text{CS}_2$  and OCS have appeared in the literature.<sup>10,11</sup> For the reactions of  $\text{M}^+ + \text{OCS}$  ( $\text{M} = \text{Fe}$  and  $\text{Co}$ ), Schwarz and co-workers determined the product cross sections for the formation of  $\text{MS}^+$ ,  $\text{MO}^+$ ,  $\text{MCS}^+$ , and  $\text{MCS}^+$ . They found that these cross sections were consistent with the initial activation of the OCS molecule by insertion of  $\text{M}^+$  into the C–S or the C–O bond to form  $\text{OC–M}^+–\text{S}$  or  $\text{O–M}^+–\text{CS}$  as intermediates.<sup>10</sup> In a more recent paper,<sup>12</sup> we reported the theoretical study of the reaction of  $\text{Fe}^+$  with  $\text{CS}_2$ , in which all observed results of the early experiment<sup>10</sup> have been rationalized. The reaction of  $\text{M}^+$  with OCS may be more complicated than that with  $\text{CS}_2$ , since there are both C–O and C–S bonds in the OCS species. The C–S bond energy (3.14 eV)<sup>13</sup> in OCS is lower than that in  $\text{CS}_2$  (4.50 eV).<sup>13,14</sup> Hence, the  $\text{MS}^+$  species can be expected to form easily from the reaction of  $\text{M}^+ + \text{OCS}$ . On the other hand, the C–S bond energy in OCS is 3.74 eV lower than the C–O bond energy (6.88 eV).<sup>13</sup> Relevant thermochemical data for the reactions of the first row transition metal ions with  $\text{CS}_2$  and OCS have been obtained experimentally,<sup>10,11</sup> but detailed information for the potential energy surfaces (PESs) of  $[\text{M}, \text{C},$

$\text{O}, \text{S}]^+$  is still scarce. Further evidence for the relevant reaction mechanisms would be forthcoming from calculations of accurate PESs. The present work presents a theoretical study of the reactivity of  $\text{Co}^+$  toward OCS. We present detailed reaction routes along both C–S and C–O bond activation branches, the relative stabilities of the initial adducts and insertion products, and the reaction barrier between the intermediates on both the triplet and quintet surfaces of  $[\text{Co}, \text{C}, \text{O}, \text{S}]^+$ . The theoretical results are compared with available experimental data.

### Calculations

The triplet and quintet PESs of  $[\text{Co}, \text{C}, \text{O}, \text{S}]^+$  for the reactions  $\text{Co}^+(\text{}^3F, 3d^8) + \text{OCS}(\text{}^1\Sigma^+)$  and  $\text{Co}^+(\text{}^5F, 4s^13d^7) + \text{OCS}(\text{}^1\Sigma^+)$ , respectively, have been considered in detail. The stationary points on the PES of  $[\text{Co}, \text{O}, \text{C}, \text{S}]^+$  were located using the B3LYP method<sup>15,16</sup> of density functional theory (DFT)<sup>17,18</sup> with a 6-311+G(d) basis set.<sup>19,20</sup> The performance of this functional has been calibrated against the experimentally known bond dissociation energies of the several species involved in the present reaction and against the results of other three functionals, B3P86, BLYP, and BP86. The harmonic vibration analyses were performed at the same level of theory for all optimized stationary points to determine their characters (minimum or first-order saddle point) and to evaluate the zero-point vibrational energies (ZPEs), which were included in all cited relative energies. The pathways between transition structures and their corresponding minima have been identified by intrinsic reaction coordinate (IRC)<sup>21</sup> calculations. The cited energies on the investigated potential energy surfaces are always given with respect to the separated ground-state species,  $\text{Co}^+(\text{}^3F) + \text{OCS}(\text{}^1\Sigma^+)$ . The present calculations were performed for both triplet and quintet surfaces of  $[\text{Co}, \text{C}, \text{O}, \text{S}]^+$  to inspect possible intersystem crossing behavior in the course of the reaction of  $\text{Co}^+$  with OCS. Our calculations include two conceivable reaction mechanisms that differ by the initial orientation of  $\text{Co}^+$  relative to the C–O or C–S bond. All calculations were performed with the Gaussian 98 program<sup>22</sup> package on an SGI Origin 2000 Server.

\* Corresponding author. E-mail: cblu@sdu.edu.cn.

**TABLE 1: Theoretical and Experimental Properties for the Ground State OCS Molecule<sup>a</sup>**

	$R_{C-S}$	$R_{C-O}$	$\omega_1$	$\omega_2$	$\omega_3$	$D_0(OC-S)^b$	$D_0(C-OS)^c$
calcd <sub>b3lyp</sub>	1.568	1.157	2115	876	512 (2)	71.5	159.8
calcd <sub>blyp</sub>	1.580	1.172	2028	842	487 (2)	75.6	164.4
calcd <sub>b3p86</sub>	1.562	1.156	2145	893	515 (2)	78.2	166.7
calcd <sub>bp86</sub>	1.575	1.171	2057	858	489 (2)	82.6	171.0
expt	1.561 <sup>d</sup>	1.156 <sup>d</sup>	2072 <sup>d</sup>	866 <sup>d</sup>	520 (2) <sup>d</sup>	71.5 <sup>e</sup>	158.2 <sup>e</sup>

<sup>a</sup> The symbols  $R$ ,  $\omega$ , and  $D_0$  denote the bond length (Å), vibrational frequencies (cm<sup>-1</sup>), and bond dissociation energies (kcal mol<sup>-1</sup>), respectively. <sup>b</sup> Calculated with respect to reaction OCS(<sup>1</sup>Σ<sup>+</sup>) → C-S(<sup>1</sup>Σ<sup>+</sup>) + O(<sup>3</sup>P). <sup>c</sup> Calculated with respect to reaction OCS(<sup>1</sup>Σ<sup>+</sup>) → C-O(<sup>1</sup>Σ<sup>+</sup>) + S(<sup>3</sup>P). <sup>d</sup> Ref 23. <sup>e</sup> Ref 24.

**TABLE 2: Theoretical and Experimental Bond Dissociation Energies at 0 K<sup>a</sup> (in eV) for Co<sup>+</sup>-O, Co<sup>+</sup>-S, Co<sup>+</sup>-CS and Co<sup>+</sup>-CO Species**

species	Co <sup>+</sup> -O	Co <sup>+</sup> -S	Co <sup>+</sup> -CS	Co <sup>+</sup> -CO
calcd <sub>b3lyp</sub>	2.75	2.63	2.82	1.69
calcd <sub>blyp</sub>	3.78	3.38	3.28	2.05
calcd <sub>b3p86</sub>	2.86	2.76	2.96	1.81
calcd <sub>bp86</sub>	3.92	3.55	3.45	2.22
expt	3.25 ± 0.05 <sup>b</sup>	2.95 ± 0.09 <sup>c</sup>	2.68 ± 0.34 <sup>c</sup>	1.80 ± 0.07 <sup>d</sup>

<sup>a</sup> With respect to Co<sup>+</sup> (<sup>3</sup>F). <sup>b</sup> Ref 25. <sup>c</sup> Ref 10. <sup>d</sup> Ref 26.

## Results and Discussion

**Evaluation of the Computational Method.** A necessary condition for obtaining a good description of the electronic states of the various species involved in the present work is the choice of a suitable level of theory with a flexible basis set. In recent years, density functional theory (DFT)<sup>17,18</sup> has attracted considerable attention and has been widely applied to electronic structure calculations for systems containing transition metals. DFT methods have been shown to be particularly useful and computationally efficient for systems with a relatively large number of electrons. Electron correlation in these systems is expected to play an important role in determining system energetics and electronic configurations. For transition metal high-spin species, such as those involved in the present reaction, calculated energies are generally very sensitive to DFT functionals utilized from the points of view of spin contamination and electron correlation. To find a reliable functional for describing the present Co<sup>+</sup> + OCS system, we calculated the molecular properties of OCS and the bond dissociation energies (BDEs) of several species involved in the reaction of Co<sup>+</sup> with OCS using several popular functionals: B3LYP, BLYP, B3P86, and BP86. The relevant results are shown in Tables 1 and 2, respectively, where available experimental values are also listed for comparison. In addition, the energies (total energies and ZPEs) of the relevant species used in deriving these BDEs are shown in Table 3. As shown in Table 1, B3LYP functional most nearly reproduced the experimental geometries, the vibrational

frequencies, and the C–O and C–S bond dissociation energies. The other three functionals gave larger errors for the bond dissociation energies, although they also predicted reasonable molecular geometries and vibrational frequencies. Table 2 compares calculated bond dissociation energies for several Co<sup>+</sup>-X (X = O, S, CO, and CS) species using the four functionals. By comparing these theoretical values with experimental findings, we found that B3LYP and B3P86 functionals gave relatively smaller absolute errors than BLYP and BP86 functionals. Discrepancies between calculated and measured values are considerable, but both B3LYP and B3P86 functionals reproduce the trend in the measured data, with the exception of Co<sup>+</sup>-CS species. The calculated results from B3LYP and B3P86 can be considered satisfactory, considering the experimental bond dissociation energy for Co<sup>+</sup>-CS is not known very accurately (the uncertainty range ± 0.34 eV). On the other hand, our main goals in the present work are the examination of the detailed reaction mechanism and the calculation of the relative energies of the species involved, not the calculation of accurate bond energies.

On the basis of the facts mentioned above, we have chosen B3LYP in view of its good capability in predicting the properties of the species involved in the reaction of Co<sup>+</sup> with OCS. The choice of B3LYP DFT method is also motivated by its extensive use in the latest literature as a practical tool in describing open-shell transition metal compounds.<sup>27,28</sup> Previous investigations on transition metal compounds<sup>29,30</sup> underlined the reliability of B3LYP for describing PESs and predicting electronic structures and thermochemical properties.

**Reactants and Products.** Experimentally,<sup>31</sup> the electronic-ground-state configuration of Co<sup>+</sup> is <sup>3</sup>F(3d<sup>8</sup>), and the first excited state <sup>5</sup>F(4s<sup>1</sup>d<sup>7</sup>) is 9.9 kcal mol<sup>-1</sup> higher in energy. It is well known that excitation energies of transition metal atoms and ions are generally difficult to compute accurately using DFT approaches.<sup>17,32</sup> In the present calculations, all the four functionals give the correct ordering of atomic states of Co<sup>+</sup>, although the excitation energy from <sup>3</sup>F to <sup>5</sup>F is overestimated by 7.4 kcal mol<sup>-1</sup> by B3LYP, 8.6 kcal mol<sup>-1</sup> by B3P86, 12.6 kcal mol<sup>-1</sup> by BLYP, and 12.7 kcal mol<sup>-1</sup> by BP86. Obviously, the energy level (17.3 kcal mol<sup>-1</sup>) calculated from B3LYP is nearest to the experimental value. It is also in fairly good agreement with Holthausen's result,<sup>33</sup> 15.1 kcal mol<sup>-1</sup>. This result supports our choice of the B3LYP functional.

The optimized structures of the various possible products on the PES of [Co, O, C, S]<sup>+</sup> are depicted in Figure 1. The superscripts denote the spin multiplicities. CS and CO are C–O and C–S bond rupture products, and their ground electronic states are <sup>1</sup>Σ<sup>+</sup>. CoS<sup>+</sup> and CoO<sup>+</sup> are predicted to have quintet ground states (<sup>5</sup>Δ, 1σ<sup>2</sup>2σ<sup>2</sup>1π<sup>4</sup>1δ<sup>3</sup>3σ<sup>1</sup>2π<sup>2</sup>), and the corresponding triplet states are higher in energy by 11.8 and 24.2 kcal mol<sup>-1</sup>, respectively. Thus ground-state products CoS<sup>+</sup> and CoO<sup>+</sup> from

**TABLE 3: Calculated Total Energies ( $E_t$ , in Hartree) and Zero-Point Vibrational Energy Energies (ZPE, in kcal mol<sup>-1</sup>) for the Species Involved in the Reaction of Co<sup>+</sup> + OCS with Different Functionals**

	B3LYP		BLYP		B3P86		BP86	
	$E_t$	ZPE	$E_t$	ZPE	$E_t$	ZPE	$E_t$	ZPE
CoO <sup>+</sup> ( <sup>5</sup> Δ)	-1457.6122690	1.09	-1457.6785530	1.14	-1458.30453607	1.13	-1457.8094974	1.18
CoS <sup>+</sup> ( <sup>5</sup> Δ)	-1780.6504287	0.60	-1780.7013383	0.64	-1781.5058915	0.63	-1780.8659825	0.67
CoCS <sup>+</sup> ( <sup>3</sup> Δ)	-1818.7749650	3.33	-1818.8128853	3.27	-1819.7349705	3.41	-1818.9875448	3.33
CoCO <sup>+</sup> ( <sup>3</sup> Δ)	-1495.8331342	4.46	-1495.8727376	4.56	-1496.6301860	4.74	-1496.0139842	4.62
OCS	-511.6001251	5.74	-511.5787887	5.50	-512.1415360	5.82	-511.6327977	5.57
CO ( <sup>1</sup> Σ <sup>+</sup> )	-113.3490503	3.16	-113.3366337	3.02	-113.5851498	3.18	-113.3463466	3.03
CS ( <sup>1</sup> Σ <sup>+</sup> )	-436.2493864	1.87	-436.2315851	1.77	-436.6479970	1.89	-436.2744997	1.79
Co <sup>+</sup> ( <sup>3</sup> F)	-1382.4197377		-1382.4584509		-1382.9758926		-1382.5837060	
O( <sup>3</sup> P)	-75.0898795		-75.0792691		-75.2215988		-75.0798011	
S ( <sup>3</sup> P)	-398.1330706		-398.1177605		-398.4275459		-398.1508105	

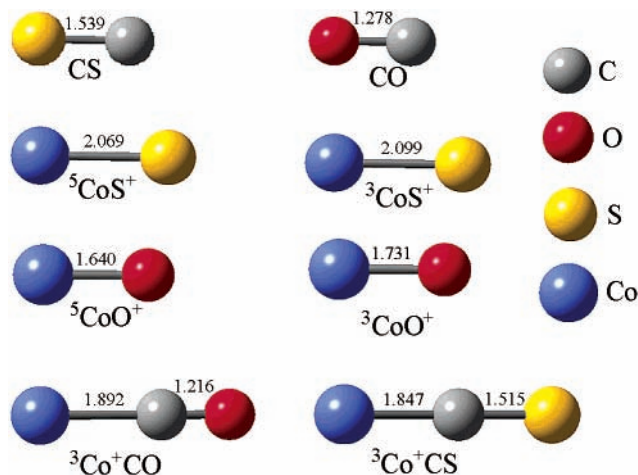


**Figure 1.** Optimized geometrical parameters for the products from the reaction of  $\text{Co}^+$  with OCS on both triplet and quintet surfaces at the B3LYP/6-311+G (d) level of theory (Distances in angstrom and angles in degrees).

reactions  $\text{Co}^+ + \text{OCS} \rightarrow \text{CoS}^+ + \text{CO}$  and  $\text{Co}^+ + \text{OCS} \rightarrow \text{CoO}^+ + \text{CS}$  are spin-forbidden on the triplet surface and spin-allowed on the quintet surface.

For products  $\text{Co}^+\text{CS}$  and  $\text{Co}^+\text{CO}$ , the predicted ground states are triplets ( ${}^3\Delta$ ), in which the highest occupied molecular orbital (HOMO) CO or CS donates electron density into the empty  $4s$  orbital of  $\text{Co}^+$  ( ${}^3F$ ,  $3d^8$ ). As shown in Figure 1, the Co–C distance in  $\text{Co}^+\text{CS}$  is smaller than that in  $\text{Co}^+\text{CO}$ , indicating the Co–C bond in the former ion is stronger than that in the latter. This is in agreement with the bond dissociation energies calculated above (Table 2).

**Initial Complexes.** As  $\text{Co}^+$  and OCS approach each other, there are two different coordination modes, which results in two possible ion-induced dipole complexes: the sulfur- and oxygen-bound structures. The computed structures for such complexes are denoted as  ${}^5\text{Co}^+-\text{SCO}^+$  and  ${}^5\text{Co}^+-\text{OCS}$  on the quintet surface, and  ${}^3\text{Co}^+-\text{SCO}$  and  ${}^3\text{Co}^+-\text{OCS}$  on the triplet surface, respectively. Their geometries are shown in Figure 2. All four complexes as well as the intermediates and transition states described hereafter were found to have  $C_s$  symmetry, their ground states are all in  $A''$  state.

For the sulfur-bound structures, the calculations predict that  ${}^3\text{Co}^+-\text{SCO}$  is 27.3 kcal mol $^{-1}$  more stable than the separate ground-state reactants, while  ${}^5\text{Co}^+-\text{SCO}$  is 31.0 less stable than  ${}^3\text{Co}^+-\text{SCO}$ . In  ${}^3\text{Co}^+-\text{SCO}$ , the OCS moiety is bound to cobalt at a distance  $r_{\text{Co}-\text{S}} = 2.299$  Å with a Co–S–C angle of 99.3°, while in  ${}^5\text{Co}^+-\text{SCO}$  these corresponding values are 2.703 Å and 101.5°, respectively. Therefore, it appears that the orbital interaction between two reactants in  ${}^3\text{Co}^+-\text{SCO}$  is stronger than in  ${}^5\text{Co}^+-\text{SCO}$ , given the shorter Co–SCO distance in the former. This is expected because the  ${}^3F$  ground state of  $\text{Co}^+$ , with its empty  $4s$  orbital, can accept the electron pair of OCS, resulting in a stronger attractive interaction ( $\pi-s$  interaction). This donation to the excited state  ${}^5F$  of  $\text{Co}^+$  is not possible, because the  $4s$  orbital is partly filled. An NBO population analysis shows the orbital population on Co to be  $4s(0.13)3d(7.98)$  for  ${}^3\text{Co}^+-\text{SCO}$ , and  $4s(1.07)3d(7.06)$  for  ${}^5\text{Co}^+-\text{SCO}$ . On the other hand, the  $3d$  electrons of  $\text{Co}^+$  can back-donate into the  $\pi^*$  orbital of the C–S bond ( $d-\pi^*$  interaction) if the distance between two reactants is close enough. One expects the  $d-\pi^*$  orbital interaction in  ${}^3\text{Co}^+-\text{SCO}$  to be more important than that in  ${}^5\text{Co}^+-\text{SCO}$ , because the Co–SCO distance in the former is smaller by 0.404 Å than that in the latter. This expectation is confirmed by the calculated  $3d$  orbital population

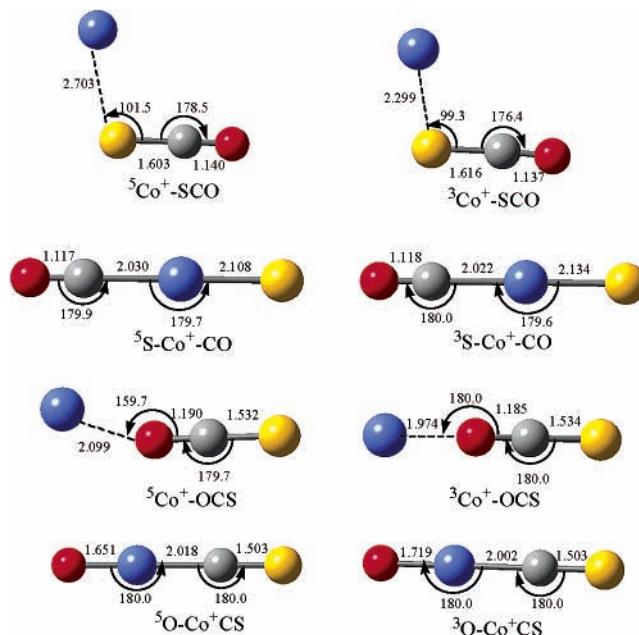


**Figure 2.** Optimized geometrical parameters for the intermediates on the PESs of  $[\text{Co}, \text{C}, \text{O}, \text{S}]^+$  of both quartet and sextet states at the B3LYP/6-311+G (d) level of theory (Distances in angstrom and angles in degrees).

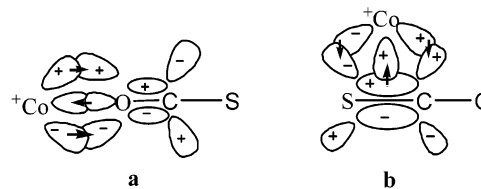


**Figure 3.** Sketch of the orbital interactions between  $\text{Co}^+$  and OCS in the initial oxygen- and sulfur-bound complexes.

(7.98 electrons) in  ${}^3\text{Co}^+-\text{SCO}$ , slightly smaller than that (8.00 electrons) for the free  ${}^3F$  state of  $\text{Co}^+$ . On the other hand, the overall  $d$  orbital population (7.06) in  ${}^5\text{Co}^+-\text{SCO}$  is even larger than that (7.00) for the free  ${}^5F$  state of  $\text{Co}^+$ . These results indicate that both the  $\pi-s$  and  $d-\pi^*$  interactions in  ${}^3\text{Co}^+-\text{SCO}$  are stronger than those in  ${}^5\text{Co}^+-\text{SCO}$ .

The ground state of the oxygen-bound encounter complex is also the triplet. This ground-bound-state complex has a linear structure with a Co–O distance of 1.974 Å, very different from that of the bent sulfur-bound encounter complex mentioned above. This fact suggests that the orbital interaction between  $\text{Co}^+$  and OCS is not same in the two initial complexes. Figs. 3a and 3b show their orbital interactions schematically. In the linear structure, the  $\sigma$  electrons of the C–O bond of OCS are transferred to the empty  $4s$  orbital of  $\text{Co}^+$ . In the bend structure, the  $\pi$  electrons of the C–S bond are transferred to the  $4s$  orbital. In both structures, the  $3d$  electrons of  $\text{Co}^+$  back-donate to  $\pi^*$  orbital of the C–O and C–S bond, respectively. From the orbital analysis shown in Figure 3, it is clear that Co in the bent structure is in a better position to insert into the C–S bond. On the other hand, the linear structure favors the direct oxygen atom abstraction. Our calculations indicate that the relative energy of this linear complex,  ${}^3\text{Co}^+-\text{OCS}$ , is 27.4 kcal mol $^{-1}$  lower than the separate ground-state reactants, which almost equals to that of the sulfur-bound encounter complex,  ${}^3\text{Co}^+-\text{SCO}$ . The corresponding quintet complex,  ${}^5\text{Co}^+-\text{OCS}$  is 23.0 kcal mol $^{-1}$  less stable than  ${}^3\text{Co}^+-\text{OCS}$ . The Co–O distance and Co–O–C angle in the quintet complex are 2.099 Å and 159.7°, respectively.



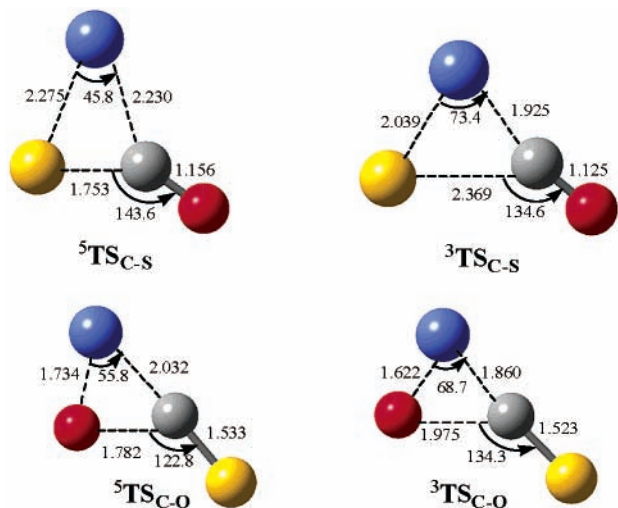


**Figure 4.** Optimized geometrical parameters for the saddle points on the PESs of  $[\text{Co}, \text{C}, \text{O}, \text{S}]^+$  of both triplet and quintet surfaces at the B3LYP/6-311+G (d) level of theory (distances in angstrom and angles in degrees).

From these encounter complexes, the C–S and C–O bonds in OCS may be activated to form various products. In the following sections, we discuss the interactions of  $\text{Co}^+$  with the C–S and C–O bonds.

**C–S Bond Activation.** Starting from the sulfur-bound encounter complex  $\text{Co}^+ \text{--} \text{SCO}$ , two C–S bond activation mechanisms can be expected. In one mechanism, the  $\text{Co}^+$  inserts into the C–S bond to form the  $\text{OC--Co}^+ \text{--} \text{S}$  intermediate, which then dissociate to form  $\text{CoS}^+$ . The other mechanism is one in which the  $\text{Co}^+$  directly abstracts the sulfur atom from OCS. The geometries of the inserted intermediates ( $^3\text{SCO}^+ \text{--} \text{CO}$ ,  $^5\text{S--Co}^+ \text{--} \text{CO}$ ) are shown in Figure 2. Clearly, both the triplet and quintet intermediates have linear structures with very similar geometry parameters. We find that the ground state of the inserted intermediate is a quintet with an energy of  $18.9 \text{ kcal mol}^{-1}$  below the ground-state reactants. The corresponding triplet intermediate is calculated to be less stable by  $9.9 \text{ kcal mol}^{-1}$ . The transformation of the encounter complex  $\text{Co}^+ \text{--} \text{SCO}$  to the inserted structure  $\text{S--Co}^+ \text{--} \text{CO}$  proceeds through the transition state called  $\text{TS}_{\text{C-S}}$  (see Figure 4), which has been confirmed by the IRC calculations. The relative energies of triplet and quintet TSs ( $^3\text{TS}_{\text{C-S}}$  and  $^5\text{TS}_{\text{C-S}}$ ) are  $4.4$  and  $24.2 \text{ kcal mol}^{-1}$  above the ground-state reactants, respectively. Structurally, the two TSs have some similarity, being three-membered-ring transition states with  $C_s$  symmetry. The imaginary frequencies are  $425i \text{ cm}^{-1}$  for  $^3\text{TS}_{\text{C-S}}$ , and  $299i$  for  $^5\text{TS}_{\text{C-S}}$ , respectively, and the normal modes correspond to the C–S bond rupture and the formations of the Co–C and Co–S bonds. In  $^3\text{TS}_{\text{C-S}}$  the breaking C–S bond is notably longer than that in the  $^5\text{TS}_{\text{C-S}}$  ( $2.369 \text{ \AA}$  for the former, and  $1.753 \text{ \AA}$  for the latter), suggesting that the triplet TS could be a late saddle point, while the quintet TS is an early one. The exit channels along the C–S bond activation branch are the direct dissociations of the insertion intermediate. There are two possible pathways: Co–S and Co–C bond ruptures, resulting in the products  $\text{CoCO}^+ + \text{S}$  and  $\text{CoS}^+ + \text{CO}$ , respectively. Our calculations indicate that these dissociation channels are barrierless. As it can be easily seen in Figure 5a, the energies of products  $\text{CoS}^+(\Delta) + \text{CO}(\Sigma^+)$ ,  $\text{CoS}^+(\Pi) + \text{CO}(\Sigma^+)$ , and  $\text{Co}^+\text{CO}(\Delta) + \text{S}(P)$  are  $10.8$ ,  $22.6$ , and  $33.4 \text{ kcal mol}^{-1}$  higher than the ground-state reactants, respectively, indicating that the Co–C bond rupture of the intermediate  $\text{S--Co}^+ \text{--} \text{CO}$  to form  $\text{CoS}^+ + \text{CO}$  is generally the most favorable exit channel. This result is in good agreement

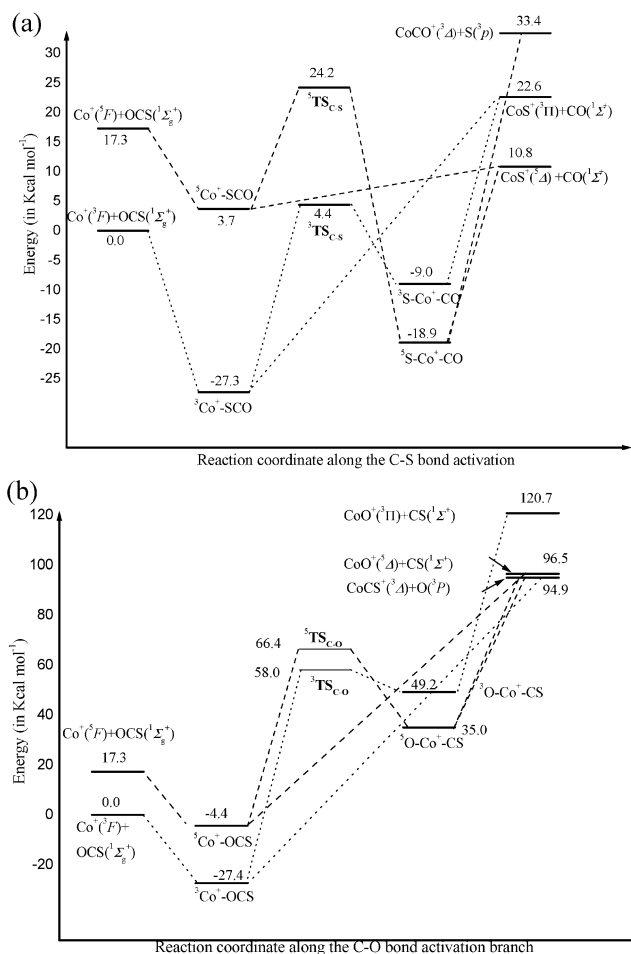


**Figure 5.** Potential energy surface profiles for the reaction of  $\text{Co}^+$  with OCS for (a) along the C–S bond activation branch and for (b) along the C–O bond activation branch. The dotted lines denote the triplet surface and the dashed lines are the corresponding quintet surface.

with the early experiment,<sup>10</sup> where the cross section for the formation of  $\text{CoS}^+$  is larger than that for  $\text{CoCO}^+$  at low energy.

From the discussion above, it is clear that the C–S bond activation involves an insertion-elimination mechanism. In addition, it might be possible that direct S atom abstraction from OCS also contributes to the observed  $\text{CoS}^+$ . All our attempts to locate a transition state of the type  $[\text{Co} \cdots \text{S} \cdots \text{C} \cdots \text{O}]^+$  either converged to the encounter complex  $\text{Co}^+ \text{--} \text{SCO}$  or collapsed into the product  $\text{CoS}^+ + \text{CO}$  on both triplet and quintet PESs during the optimization, indicating that there is no tight transition state structure for the direct abstraction reaction.

The energy profile along the C–S bond activation branch from the reaction of  $\text{Co}^+$  with OCS is summarized in Figure 5a. It is clearly shown that the initial triplet complex  $^3\text{Co}^+ \text{--} \text{SCO}$  is the global minimum along the C–S bond activation branch on the PES of  $[\text{Co}, \text{C}, \text{O}, \text{S}]^+$ . Because the ground state of the inserted species is quintet, one must consider the possibility that spin–orbit interaction causes hopping from the triplet surface to the quintet surface. It is well known that transition metal mediated reactions very often occur on more than only one PES.<sup>34</sup> For the present system, the spin–orbit interaction is very likely large enough to allow for an efficient conversion to energetically most favorable surface along the reaction coordinate.

**C–O Bond Activation.** The intermediates and transition states involved along the C–O bond activation branch are again shown in Figures 2 and 4, respectively, while the energy profile

is shown in Figure 5b. Similar to the C–S bond activation, the mechanism for C–O activation is found to be also an insertion–elimination process. The present calculations show no evidence for the direct O atom abstraction by  $\text{Co}^+$  from OCS. The structures of the C–O bond inserted intermediates are similar to the corresponding C–S inserted intermediates. The ground state of this intermediate is quintet, and its energy was calculated to be 35.0 kcal mol<sup>-1</sup> above the ground-state reactants. The corresponding triplet is higher in energy by 14.2 kcal mol<sup>-1</sup>. These C–O bond inserted intermediates  $^5\text{O–Co}^+–\text{CS}$  and  $^3\text{O–Co}^+–\text{CS}$  are energetically much less favorable than the corresponding C–S bond inserted products  $^5\text{S–Co}^+–\text{CO}$  and  $^3\text{S–Co}^+–\text{CO}$  (cf. Figure 5). The initial complex  $\text{Co}^+–\text{OCS}$  and the inserted intermediate  $\text{O–Co}^+–\text{CS}$  are connected by  $\text{TS}_{\text{C–O}}$ , a first-order saddle point of the C–O bond activation. The energies of the triplet and quintet TSSs,  $^3\text{TS}_{\text{C–O}}$  and  $^5\text{TS}_{\text{C–O}}$ , are located at 58.0 and 66.4 kcal mol<sup>-1</sup> above the ground-state reactants, respectively, and the corresponding imaginary frequencies are 589i and 415i. When comparing Figure 5a with Figure 5b, we noted that the energy barriers for the C–O bond activation on both triplet and quintet PESs are much higher than the corresponding PESs of the C–S bond activation, suggesting the C–O bond activation is much less favorable than the C–S bond activation. Similarly to  $\text{S–Co}^+–\text{CO}$ , there are two possible dissociation channels from intermediate  $\text{O–Co}^+–\text{CS}$ : the Co–C bond rupture to form  $\text{CoO}^+$  and CS, and the Co–O bond rupture to form  $\text{CoCS}^+$  and an O atom. Our calculations show that the three product channels  $\text{Co}^+ + \text{CS}(^3\Delta) + \text{O}(^3P)$ ,  $\text{CoO}^+(^5\Delta) + \text{CS}(^1\Sigma^+)$ , and  $\text{CoO}^+(^3\Pi) + \text{CS}(^1\Sigma^+)$  are endothermic by 94.9, 96.5, and 120.7 kcal mol<sup>-1</sup>, respectively. The PES profile of the C–O bond activation branch is similar to that of the C–S bond activation branch: the initial triplet adduct is the global minimum along this branch, and the ground state of the C–O bond inserted intermediate is quintet. Thus, spin–orbit interaction may also be important in determining the outcome of reactions which proceed via C–O bond activation.

## Conclusion

The reactivity of  $\text{Co}^+$  toward OCS on both triplet and quintet surfaces has been studied at the B3LYP/6-311+G(d) level of theory. The calculations provide a detailed picture of the C–S and C–O bond activations in OCS mediated by a bare  $\text{Co}^+$  ion. Both the C–S and C–O bond activations proceed via the insertion–elimination mechanism. The direct sulfur and oxygen atom abstractions by  $\text{Co}^+$  might contribute to the formation of  $\text{CoS}^+$  and  $\text{CoO}^+$ . However, tight transition state structures for the activation pathways were not found in the present calculations. The theoretical results show that the C–S bond activation, which results in products  $\text{CoS}^+$  and  $\text{CoCO}^+$ , is energetically less demanding than the C–O activation, which results in products  $\text{CoO}^+$  and  $\text{CoCS}^+$ . The present calculations support the findings of the early experiment.<sup>10</sup> The ground states of  $\text{CoS}^+$  and  $\text{CoO}^+$  are quintet states, while the ground states  $\text{CoCO}^+$  and  $\text{CoCS}^+$  are triplet. Intersystem crossing between the triplet and quintet surfaces of  $[\text{Co}, \text{C}, \text{O}, \text{S}]^+$  is likely to occur during the course of  $\text{Co}^+$  insertion into the C–S or C–O bond.

**Acknowledgment.** We gratefully acknowledge the reviewers for many constructive comments. This work was fully supported by the National Natural Science Foundation of China (No.: 20073024).

## References and Notes

- (1) Stiefel, E. I., In *Transition Metal Sulfur Chemistry*; E. I. Stiefel, K. Matsumoto, Eds.; ACS Symposium Series 653. American Chemical Society: Washington, DC, 1996.
- (2) Pandey, K. K. *Coord. Chem. Rev.* **1995**, *140*, 37.
- (3) Takakuwa, S. In *Organic Sulfur Chemistry, Biochemical Aspects*; Oae, S., Okyama, T., Eds.; CRC Press: Boca Raton, FL, 1992; p 1.
- (4) Holm, R. H. *Chem. Rev.* **1996**, *96*, 2237.
- (5) Kaim, W.; Schwederski, B. *Bioinorganic Chemistry: Inorganic Elements in the Chemistry of Life*; Wiley & Sons: New York, 1994.
- (6) Kondo, T.; Mitsudo, T. *Chem. Rev.* **2000**, *100*, 3205.
- (7) Almond, M.; Cockayne, B.; Cooke, S. A.; Pice, D. A.; Smith, P. C.; Wright, P. J. *J. Mater. Chem.* **1996**, *6*, 1639.
- (8) Butler, I. S.; Fenster, A. E. *J. Organomet. Chem.* **1974**, *66*, 161.
- (9) Broadhurst, P. V.; Leadbeater, N. E.; Lewis, J.; Raithby, P. R. *J. Chem. Soc., Dalton Trans.* **1997**, *23*, 4579.
- (10) Rue, C.; Armentrout, P. B.; Kretzschmar, I.; Schroder, D.; Schwarz, H. *J. Phys. Chem. A*, **2001**, *105*, 8456.
- (11) Rue, C.; Armentrout, P. B.; Kretzschmar, I.; Schroder, D.; Schwarz, H. *J. Phys. Chem. A* **2002**, *106*, 9788.
- (12) Jiang, N.; Zhang, D. *J. Chem. Phys. Lett.* **2002**, *366*, 253.
- (13) Pedley, J. B.; Naylor, R. D.; Kirby, S. P. *Thermochemical Data of Organic Compounds*; Chapman and Hall: London, 1986.
- (14) Prinslow, D. A.; Armentrout, P. B. *J. Chem. Phys.* **1991**, *94*, 3563.
- (15) Becke, A. D. *J. Chem. Phys.* **1993**, *98*, 1372.
- (16) Lee, C.; Yang, W.; Parr, R. G. *Phys. Rev. B* **1988**, *37*, 785.
- (17) Parr, R. G.; Yang, W. *Density Functional Theory of Atom and Molecules*; Oxford University Press: Oxford, 1989.
- (18) Kryachko, E. S.; Ludena, E. V. *Electron Density Functional Theory of Many-Electron Systems*; Kluwer: Dordrecht, 1990.
- (19) McLean, A. D.; Chandler, G. S. *J. Chem. Phys.* **1980**, *72*, 5639.
- (20) Hay, P. J. *J. Chem. Phys.* **1977**, *66*, 4377.
- (21) Gonzalez, C.; Schlegel, H. B. *J. Phys. Chem.* **1990**, *94*, 5523.
- (22) Frisch, M. J.; Trucks, G. W.; Schlegel, H. B.; Scuseria, G. E.; Robb, M. A.; Cheeseman, J. R.; Zakrzewski, V. G.; Montgomery, J. A., Jr.; Stratmann, R. E.; Burant, J. C.; Dapprich, S.; Millam, J. M.; Daniels, A. D.; Kudin, K. N.; Strain, M. C.; Farkas, O.; Tomasi, J.; Barone, V.; Cossi, M.; Cammi, R.; Mennucci, B.; Pomelli, C.; Adamo, C.; Clifford, S.; Ochterski, J.; Petersson, G. A.; Ayala, P. Y.; Cui, Q.; Morokuma, K.; Malick, D. K.; Rabuck, A. D.; Raghavachari, K.; Foresman, J. B.; Cioslowski, J.; Ortiz, J. V.; Stefanov, B. B.; Liu, G.; Liashenko, A.; Piskorz, P.; Komaromi, I.; Gomperts, R.; Martin, R. L.; Fox, D. J.; Keith, T.; Al-Laham, M. A.; Peng, C. Y.; Nanayakkara, A.; Gonzalez, C.; Challacombe, M.; Gill, P. M. W.; Johnson, B. G.; Chen, W.; Wong, M. W.; Andres, J. L.; Head-Gordon, M.; Replogle, E. S.; Pople, J. A. *Gaussian 98*, revision A.9; Gaussian, Inc.: Pittsburgh, PA, 1998.
- (23) Lahaye, J. G.; Vandenhoute, R.; Fayt, A. *J. Mol. Spectrosc.* **1987**, *123*, 48.
- (24) Chase, M. W., Jr.; Davies, A. C.; Downey, J. R., Jr.; Fruirip, D. J.; McDonald, R. A.; Syverud, A. N. *JANAF Tables, J. Phys. Chem. Ref. Data* **1985**, *11*, Suppl. 1.
- (25) Loh, S. K.; Fisher, E. R.; Lian, L.; Schultz, R. H.; Armentrout, P. B. *J. Phys. Chem.* **1989**, *93*, 3159.
- (26) Goebel, S.; Haynes, C. L.; Khan, F. A.; Armentrout, P. B. *J. Am. Chem. Soc.* **1995**, *117*, 6994.
- (27) Pavlov, M.; Siegbahn, P. E.; Sandstrom, M. *J. Phys. Chem. A* **1998**, *102*, 219.
- (28) Peschke, M.; Blades, A. T.; Kebarle, P. *J. Am. Chem. Soc.* **2000**, *122*, 1492.
- (29) Davidson, E. R. *Chem. Rev.* **2000**, *100*, 351.
- (30) Pavlov, M.; Siegbahn, P. E. M.; Sandstrom, M. *J. Phys. Chem. A* **1998**, *102*, 219.
- (31) Statistical average over all *J* levels. Energies taken from the following: Moore, C. E. *Atomic energy level*. Natl. Bur. Stand. (U. S.), Circ. 467: Washington, DC, 1949.
- (32) Morre, C. E. *Atomic Energy Levels*; NSRD-NBS, USA.; US Government Printing Office: Washington, DC, 1991; Vol. 1.
- (33) Holthausen, M. C.; Koch, W. *J. Am. Chem. Soc.* **1996**, *118*, 9932.
- (34) Shaik, S.; Danovich, D.; Fiedler, A.; Schroder, D.; Schwarz, H. *Helv. Chim. Acta* **1995**, *78*, 1393.